RESEARCH ARTICLE doi.org/10.1002/adsc.70035

Check for updates

ADVANCED SYNTHESIS & CATALYSIS

Harnessing Vinylogy with Radicals: Photoinduced γ-Benzylation Reactions of 2-Silyloxyfurans

Enrico Marcantonio,[a,b] Debora Guazzetti,[a] Luca Aimi,[a] Kelly Bugatti,[a] Pedro Mena,[c] Marco Giannetto,[d] Simone Fortunati,[d] Andrea Sartori,[a] Lucia Battistini,[a] Leonardo Andreoni,[e,f] Marco Lombardo,[g] Franca Zanardi,[a,*] and Claudio Curti[a,*]

[a] Department of Food and Drug, University of Parma, Parco Area delle Scienze 27A, I-43124 Parma, Italy
E-mail: franca.zanardi@unipr.it; claudio.curti@unipr.it
[b] Department of Chemistry, Aarhus University, 8000 Aarhus, Denmark
[c] Department of Food and Drug, University of Parma, Via Volturno 39, I-43125 Parma, Italy
[d] Department of Chemistry, Life Sciences and Environmental Sustainability, University of Parma, Parco Area delle Scienze 17A, 43124 Parma, Italy
[e] Department of Industrial Chemistry "Toso Montanari", University of Bologna, Via Gobetti 85, 40129 Bologna, Italy
[f] CLAN-Center for Light Activated Nanostructures, Istituto ISOF-CNR, via Gobetti 101, 40129 Bologna, Italy
[g] Department of Chemistry "Giacomo Ciamician", University of Bologna, Via P. Gobetti 85, 40129 Bologna, Italy

Manuscript received: May 8, 2025; Revised manuscript received: June 23, 2025;
Version of record online: July 17, 2025

Supporting information for this article is available on the WWW under https://doi.org/10.1002/adsc.70035

© 2025 The Author(s). Advanced Synthesis & Catalysis published by Wiley-VCH GmbH. This is an open access article under the terms of the Creative Commons Attribution License, which permits use, distribution and reproduction in any medium, provided the original work is properly cited.

Abstract: 2-Silyloxyfurans are among the most exploited Mukaiyama-type vinylogous nucleophiles from which a myriad of bioactive γ-butyrolactones have been accessed. Although a plethora of "polar" reactions featuring this scaffold as a key player have been developed so far, its behavior in radical chemistry is still in its infancy. Herein, the development of two complementary vinylogous, radical-mediated benzylations of 2-silyloxyfurans, promoted by visible light and suitable photoredox catalysts, is described. Common to both photocatalytic cycles is the reduction of a suitable redox active ester forging a key benzyl radical intermediate, which undergoes two different fates. First, the photoinduced oxidation of the silyloxyfuran generates an unprecedented silyl-radical cation species able to trap the nucleophilic benzyl radical. Alternatively, with specific electron-rich substrates, the benzyl radical can be converted to the corresponding benzyl carbocation intermediate via a net-neutral radical-polar crossover pathway, enabling a vinylogous, polar benzylation reaction. A broad scope of chiral, γ-benzyl butenolides is obtained in one step, some of which are used as strategic precursors to access bioactive phenyl-γ-valerolactone metabolites.

Keywords: benzyl radical, lactones, photoredox catalysis, principle of vinylogy, radical-polar crossover

1. Introduction

Since their first appearance in the mid-70s,[1] 2-silyloxyfurans **1** (the extended silylketene acetals of furan-2(5H)one **I**, **Figure 1A**) have become among the most exploited Mukaiyama-type vinylogous nucleophiles.[2] These scaffolds are invaluable starting materials from which a myriad of densely functionalized chiral butenolides and butyrolactones have been constructed.[3] Of note, the silicon moiety in dienolate **1** provides stability while also imparting increased highest occupied molecular orbital (HOMO) at the remote γ-position of the electron-rich furan ring; this favors its remote γ-C(sp^2)–H functionalization with a plethora of electrophiles, including C(sp^2)-centered representatives, hence forging novel and valuable C–C

 © 2025 The Author(s). Advanced Synthesis & Catalysis published by Wiley-VCH GmbH

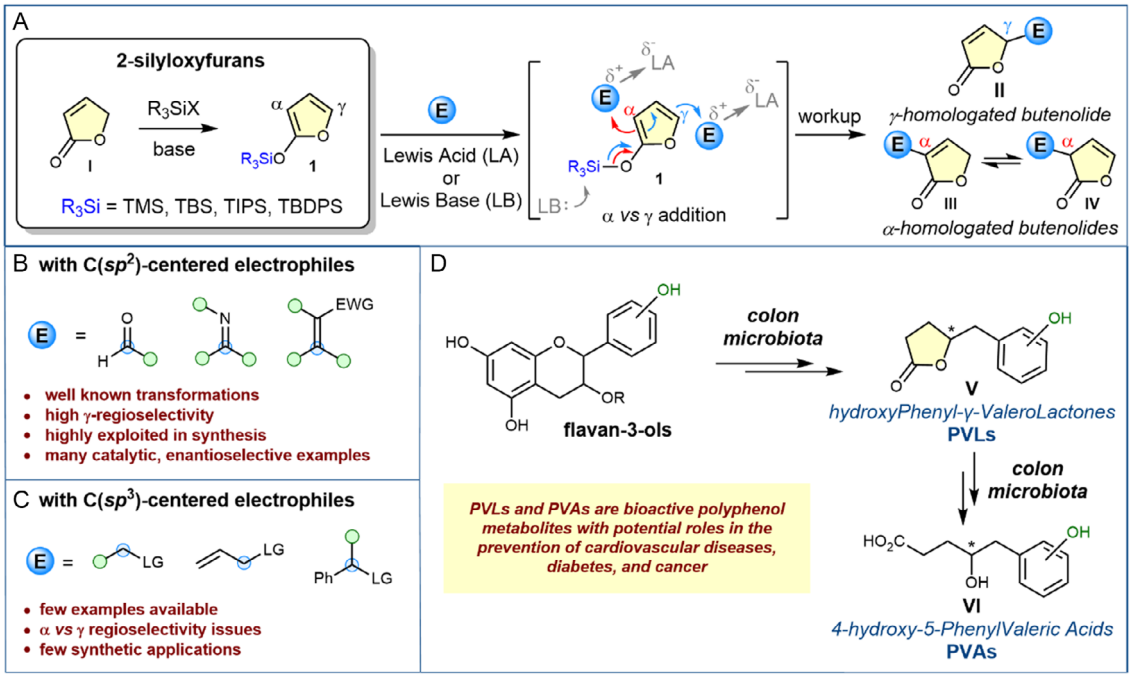

Figure 1. A–C) The "polar" vinylogous addition of 2-silyloxyfurans **1** to carbon-centered electrophiles **E**. D) Hydroxyphenyl γ-valerolactones and their 4-hydroxy-5-phenylvaleric acid derivatives as the main colonic metabolites of dietary flavan-3-ols.

linkages (Figure 1A,B).[2] This behavior has elevated such cyclic silyl dienolates to a prominent role in evergreen "polar" transformations, such as the vinylogous Mukaiyama aldol, Mannich, and Michael addition reactions, declined in a diverse toolbox of regio-, diastereo- and enantioselective variants.[4]

Among the first and most studied transformations of nonvinylogous (silyl)enolates is their α-alkylation reaction with primary or secondary C(sp^3)-centered electrophiles like alkyl/allyl halides, thereby forming novel C─C bonds adjacent to the carbonyl group (Figure 1C).[5] Surprisingly, the vinylogous extension of such reactions is highly underrepresented, and mostly limited to transition metal-catalyzed allylic alkylation reactions.[6] This void is quite unexpected since the streamlined alkylation of **1** with suitable C(sp^3)-centered alkyl electrophiles would in principle provide quick access to the α- or γ-alkyl butenolides **II**, **III**, or **IV** (Figure 1A) and their saturated butyrolactone congeners, which constitute the structural core of many natural products and pharmaceuticals displaying an impressive range of biological activities.[7] Among these, hydroxyphenyl-γ-valerolactones of type **V** (PVLs, Figure 1D), a family of chiral compounds featuring a butyrolactone core bearing a (poly)hydroxylated benzyl side chain at C5, have risen to prominence in food science and nutrition.[8] PVLs and their corresponding open-ring 4-hydroxy-5-phenylvaleric acid derivatives **VI** (PVAs) were found as the main colonic metabolites of flavan-3-ols, the major class of flavonoids in the human diet, and increasing research evidence attributes to these scaffolds potential roles in the prevention of cardiovascular diseases, diabetes, and cancer. On these premises, the development of general, catalytic methods for the direct alkylation of prochiral, vinylogous silyl ketene acetals represents an ongoing challenge in organic synthesis. Besides these HOMO-driven polar transformations, enol silanes have also been exploited as versatile platforms in radical chemistry,[9] behaving essentially as 1) electron-rich, nucleophilic singly occupied molecular orbital (SOMO)-phile reagents capable of intercepting electrophilic radicals (**Scheme 1A**),[10] or 2) as readily available radical-cation precursors via chemical ([O]) or photoinduced electron transfer (PET) oxidation, promoted by either photosensitization or photoredox catalysis (Scheme 1B).[11]

Indeed, silyl enol ethers and silyl ketene acetals are known to be easily oxidizable organic substrates, with $E^0_{1/2}$ for oxidation ranging from +0.8 to +1.3 V (in MeCN vs saturated calomel electrode (SCE)).[12] Such bias enables their oxidation by single-electron transfer quite easily, affording the corresponding silyl radical-cation intermediates **VII** (Scheme 1B). These species may then either react as such, as strongly electrophilic radicals or, more commonly, as α-keto radicals **VIII**, after desilylation under suitable conditions.[13] Once formed, electrophilic radicals **VII** or **VIII** may react either with other radical species via radical–radical coupling, or couple with suitable electron-rich SOMO-phile reagents, to afford the corresponding α-alkyl adducts

© 2025 The Author(s). Advanced Synthesis & Catalysis published by Wiley-VCH GmbH

16154169, 2025, 16, Downloaded from https://advanced.onlinelibrary.wiley.com/doi/10.1002/adsc.70035 by CochraneItalia, Wiley Online Library on [13/01/2026]. See the Terms and Conditions (https://onlinelibrary.wiley.com/terms-and-conditions) on Wiley Online Library for rules of use; OA articles are governed by the applicable Creative Commons License

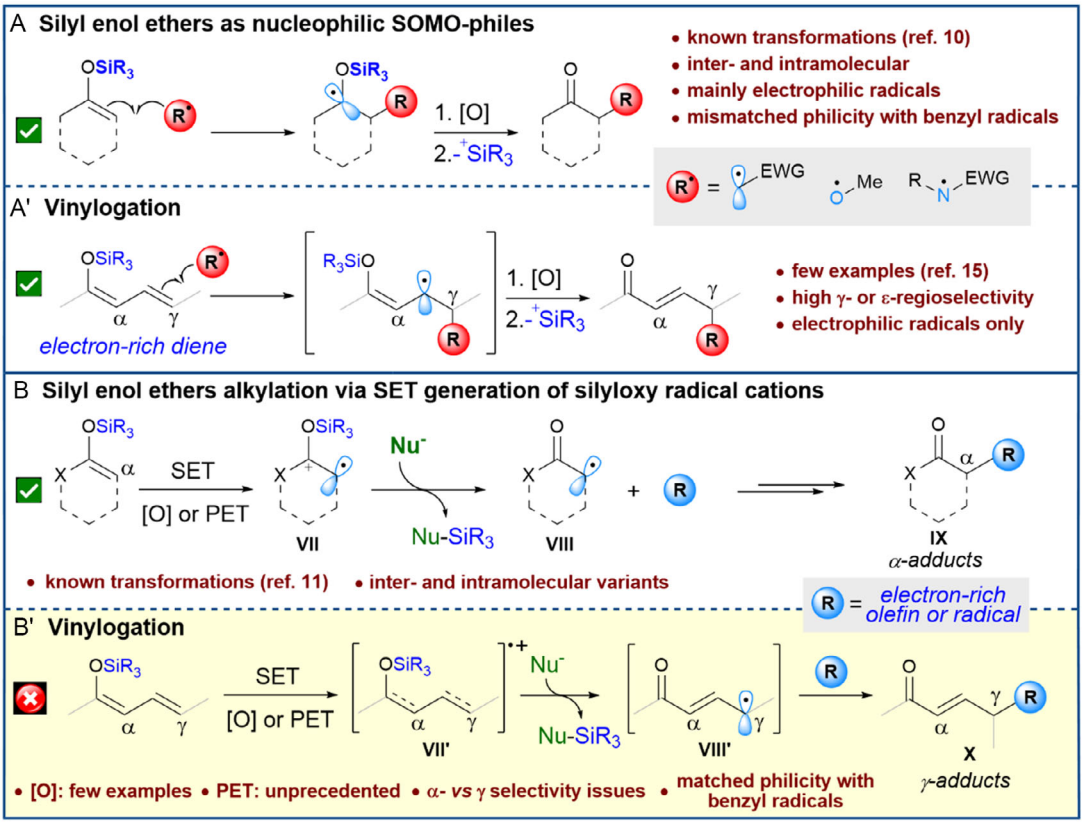

Scheme 1. A–A′) Silyl (poly)enol ethers as nucleophilic SOMO-philes. B–B′) Silyl (poly)enol ethers as electrophilic radical-cation precursors.

IX.[14] While few notable examples have recently appeared, dealing with coupling of silyl (poly)enol ethers with electrophilic radicals (Scheme 1A′),[15] to the best of our knowledge, vinylogous reactions based on PET oxidation of extended silyl (poly)enolates are still unprecedented (Scheme 1B′).[15d] In this instance, the envisioned photoinduced oxidation would generate the corresponding (silyl)radical cations **VII**′ (or their desilylated counterparts **VIII**′) which might couple with suitable electron-rich olefins or C-centered radicals to afford the corresponding γ-alkyl adducts **X**, hence expanding the uncharted chemical space of accessible products, and opening challenging yet intriguing α versus γ regioselectivity issues. Focusing on furan **1** as a privileged vinylogous electron-rich silyloxydiene system, its ability to directly engage benzyl radicals via the pathway depicted in Scheme 1A′ would be rewarding yet highly challenging since both diene **1** and the benzylic radical possess the same "nucleophilic behavior" (a sort of philicity mismatch).[16] To override this "philicity issue," the general option presented in Scheme 1B′ could be applied to **1**, by promoting a radical–radical cross-coupling between the (silyl) radical cation $\mathbf{1}^{\bullet+}$, generated in situ via PET oxidation of **1**, and a suitable benzyl radical counterpart $\mathbf{2}^{\bullet}$ (**Scheme 2**).[11,17]

With this in mind, we sought to develop novel catalytic, vinylogous alkylation reactions with suitable benzyl radical precursors by exploiting a PET strategy on vinylogous silyloxyfurans **1**. Herein, we showcase the fulfillment of this idea unveiling a novel protocol (here called Protocol A) of a vinylogous, radical benzylation reaction between silyloxyfurans **1** and *N*-(arylacetoxy) phthalimides **2** (NHPI esters)[18] as key precursors of benzyl radical intermediates $\mathbf{2}^{\bullet}$ (Scheme 2A).[19] Furthermore, surveying specific electron-rich benzyl radicals $\mathbf{2}^{\bullet}$, which are prone to be converted to the corresponding benzyl carbocations $\mathbf{2}^{+}$, a second, complementary protocol could be disclosed (Protocol B, Scheme 2C). Here, a net-neutral radical polar crossover pathway[20] enabled an unprecedented vinylogous polar alkylation reaction. Both strategies proved successful and enabled access to chiral γ-benzyl butenolides of type **3** in one step, some of which were used as strategic precursors of bioactive phenyl-γ-valerolactone metabolites.

2. Results and Discussion

2.1. Protocol A: Reaction Development

To prove the feasibility of our idea, we choose triisopropylsilyloxyfuran (TIPSOF, **1a**) and *N*-(phenylacetoxy)

© 2025 The Author(s). Advanced Synthesis & Catalysis published by Wiley-VCH GmbH

16154169, 2025, 16, Downloaded from https://advanced.onlinelibrary.wiley.com/doi/10.1002/adsc.70035 by CochraneItalia, Wiley Online Library on [13/01/2026]. See the Terms and Conditions (https://onlinelibrary.wiley.com/terms-and-conditions) on Wiley Online Library for rules of use; OA articles are governed by the applicable Creative Commons License

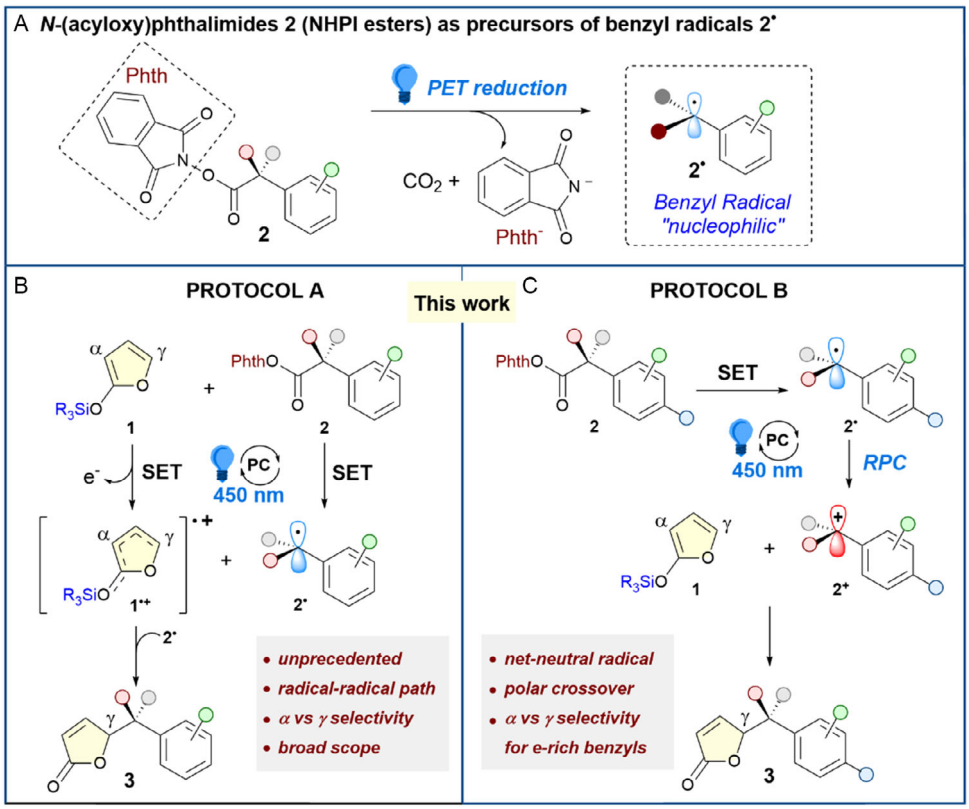

Scheme 2. A) NHPI esters as benzyl radical precursors. B,C) This work: photoinduced γ-benzylations of 2-silyloxyfurans **1** with benzyl NHPIs **2** via Protocol A and Protocol B.

phthalimide **2a** in a 1:2 ratio as model substrates (**Table 1**). Initially, we tested the reaction using 2.5 mol% of Ir(dF-CF_3-ppy)$_2$(dtbpy)PF_6 (**Ir-1**), a known photocatalyst potentially capable of oxidizing **1** to its sought radical-cation intermediate [$E^*_{ox} = +1.21$ V vs SCE].[21] Under blue-light irradiation, in degassed MeCN, at 30 °C for 16 h, the reaction provided a crude whose ^{1}H-NMR spectrum revealed the formation of the expected γ-adduct **3aa**, and minor amounts of two tautomeric α-adducts, *iso*-**4aa** and **4aa**, in a 1:0.1:0.4 ratio and in a 50% combined NMR yield (Table 1, entry 1). Other oxidizing metal- and organophotocatalysts proved competent in this model reaction, even though no improvements in the overall yield and regioselectivity were observed (entries 2–3, see also Table S1, Supporting Information). Also, different silyloxyfurans other than **1a** were evaluated under the same reaction conditions without improvements: in fact, while the use of the less hindered trimethylsilyloxyfuran **1b** resulted in the recovery of desilylated starting materials (entry 4), the *tert*-butyldimethylsilyl congener **1c** operated similarly, but not better than **1a** giving access to **3aa** with a combined yield of 40% (Table 1, entry 5). As for the solvent, an in-depth screening of various options was performed (see Table S2, Supporting Information), and degassed MeCN resulted the best choice in terms of both efficiency and regioselectivity. The use of deuterated CD_3CN (48% yield, entry 6) instead of MeCN did not affect the efficiency of reaction, while adding water as an activator of RAEs **2**,[22] failed to improve our process, affording a 1:0.2:0.3 mixture of products (**3aa**:*iso*-**4aa**:**4aa**) with a meagre 31% combined yield (entry 7). We also found that the presence of basic additives such as DIPEA (5 mol%) or a raise of reaction temperature up to +45 °C proved detrimental to the reaction outcome (entries 8 and 9). During this survey, we were challenged by the presence of a series of by-products in the reaction crudes, whose ratio was scarcely reproducible. As a hint of the radical process, we were able to identify them as *meso*-furan-2(5H) one γ,γ′-bis adduct **5a** and (±)-**5b** (typically as 1:1 diastereomeric mixture),[23] diphenylethane **6** (likely derived by homocoupling of benzyl radicals), and the residual phthalimide **7** (see Figure S3 and S4, Supporting Information). The formation of these by-products proved detrimental to the efficiency of the reaction, so we moved on trying to reduce their presence. Shortening the reaction time from 16 to 2 h allowed to reduce the level of by-products in favor of a 1:0.5 **3aa**/*iso*-**4aa** mixture (free from **4aa**) in a 62% yield (entry 10).

Interestingly, after purification of the crude via flash chromatography, only pure **3aa** and **4aa** (in a 1:0.5 ratio)

© 2025 The Author(s). Advanced Synthesis & Catalysis published by Wiley-VCH GmbH

16154169, 2025, 16, Downloaded from https://advanced.onlinelibrary.wiley.com/doi/10.1002/adsc.70035 by CochraneItalia, Wiley Online Library on [13/01/2026]. See the Terms and Conditions (https://onlinelibrary.wiley.com/terms-and-conditions) on Wiley Online Library for rules of use; OA articles are governed by the applicable Creative Commons License

Table 1. Protocol A: optimization of reaction conditions (selected entries).

Entry[a]	Deviations from the initial conditions	Yield [%][b]	r.r.[c] **3aa**:*iso*-**4aa**:**4aa**
1	None	50 (32)	1:0.1:0.4
2	*fac*-Ir(ppy)$_3$ (**Ir-2**)	<5	n.d.
3	Ir(ppy)$_2$(dtbpy)PF$_6$ (**Ir-3**)	35	1:0:0.3
4	**1b** instead of **1a**	<5	n.d.
5	**1c** instead of **1a**	40	1:0.1:0.4
6	CD_3CN as solvent	48	1:0.1:0.4
7	+H_2O (25 equiv)	31	1:0.2:0.3
8	+DIPEA (5 mol%)	29	1:0:0.6
9	45 °C	38	1:0.2:0.3
10	2 h reaction time	62 (43)	1:0.5:0
11	2 equiv. **1a**, 1 equiv. **2a**; 2 h	75 (50)	1:0.5:0
12[d]	No photocatalyst nor light	0	n.d.

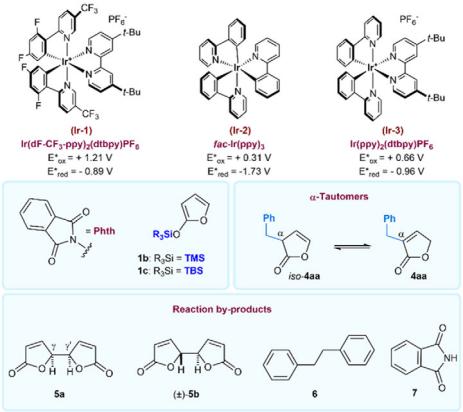

[a] Initial reaction conditions: **1a** (0.07 mmol), **2a** (0.14 mmol, 2.0 equiv), and **Ir-1** (2.5 mol%) in degassed MeCN [0.07M] at 30 °C, irradiated with blue LEDs (450 nm) for 16 h;
[b] Combined NMR yield determined by ^{1}H NMR analysis of the crude with trimethylorthoformate as internal standard. Isolated yield of pure **3aa** in parentheses;
[c] Regioisomeric ratio (r.r.) determined by ^{1}H NMR of the crude;
[d] Reactions performed independently without blue LEDs or without photocatalyst. n.d. = not determined. For details, see Table S1–S5, Supporting Information.

could be isolated (60% combined yield, 43% pure **3aa**) entailing a favorable switch of the unconjugated butenolide *iso*-**4aa** to its conjugated tautomer **4aa**. We solved the overall issue by adjusting the molar ratio between **1a** and **2a**: using a 2:1 mixture of **1a** and **2a** in MeCN at 30 °C for 2 h, a 1:0.5 **3aa**/*iso*-**4aa** mixture with an optimal 75% combined NMR yield was afforded, secured by the isolation of pure **3aa** and **4aa** after column chromatography with almost the same efficiency (entry 11). Of note, pure γ-benzylated adduct was isolated as a single regioisomer in a satisfactory 50% yield. Finally, control experiments revealed that both light and photocatalyst were necessary to generate the products (entry 12).

2.2. Protocol A: Evaluation of Substrate Scope

With the optimal conditions at hand, we next probed the generality of the reaction scope (**Scheme 3**). To face this task, we commenced with the synthesis of a panel of differently functionalized *N*-(arylacetoxy)phthalimides **2**, which were readily available from the corresponding carboxylic acids and *N*-hydroxyphthalimide via a slightly modified literature procedure (see Representative Procedure A in the Supporting Information).

We began surveying both electron-deficient and electron-rich *para*-substituted NHPI esters which proved to be competent radical precursors under the optimized reaction conditions. Indeed, the corresponding adducts **3ab-3ag** were obtained in good overall yields, with the (4-*tert*-butyl)benzyl derivative **3af** being the best entry (85% combined yield of a 2:1 γ:α regioisomeric mixture; 57% isolated yield of the pure γ-adduct). Both *ortho*- and *meta*-substituted derivatives behaved similarly, furnishing up to 2:1 γ:α mixtures of products **3aj-3an** in moderate to good 50–73% combined yields (30–55% of pure γ-adducts). However, 4-methoxybenzyl- and 4-phenoxybenzyl derivatives **3ah** and **3ai** deviated from this trend, providing the corresponding adducts in meagre 30–35% combined yields. Interestingly, a thiophene-based derivative **3ao** was also accessible with comparable results, with a good 43% of pure γ-adduct obtained after chromatographic purification of the crude. We next moved to test secondary and tertiary benzyl radical precursors. Again, both prostereogenic (methyl) benzyl precursor and the tertiary (dimethyl)benzyl congener proved viable under the optimized reaction conditions, yielding the corresponding adducts **3ap** and **3aq** in good yields and regioselectivities, albeit the former was isolated as an inseparable 1:1 diastereomeric mixture. Similar behavior was also exerted by a drug-like scaffold such as ibuprofen derivative **2r**, which provided the corresponding adduct **3ar** in a moderate 45% combined yield as a 2:1 γ:α mixture. A couple of reactions (e.g., **3aa** and **3af**) were also scaled up on a 3 mmol scale (≈0.8 g) without detriment of both efficiency and regioselectivity. Furthermore, we tested γ- and α-methyl-substituted silyloxyfurans **1d** and **1e**, readily available respectively from α-angelicalactone and 3-methyl-2(5H)-furanone using standard conditions (see Section S2.2, Supporting Information). Under the optimized reaction conditions, both scaffolds reacted with **2a** with similar efficiency (48–63% combined NMR yields), albeit with opposite regioselectivity; indeed, γ-methyl silyloxyfuran **1d** reacted with **2a** to give a slight excess of α-adduct **4da** (1:1.2 **3da**:**4da**), while its α-methyl congener **1e** provided the γ-adduct **3ea** preferably (3.5:1 **3ea**:**4ea**). Finally, the

© 2025 The Author(s). Advanced Synthesis & Catalysis published by Wiley-VCH GmbH

16154169, 2025, 16, Downloaded from https://advanced.onlinelibrary.wiley.com/doi/10.1002/adsc.70035 by CochraneItalia, Wiley Online Library on [13/01/2026]. See the Terms and Conditions (https://onlinelibrary.wiley.com/terms-and-conditions) on Wiley Online Library for rules of use; OA articles are governed by the applicable Creative Commons License

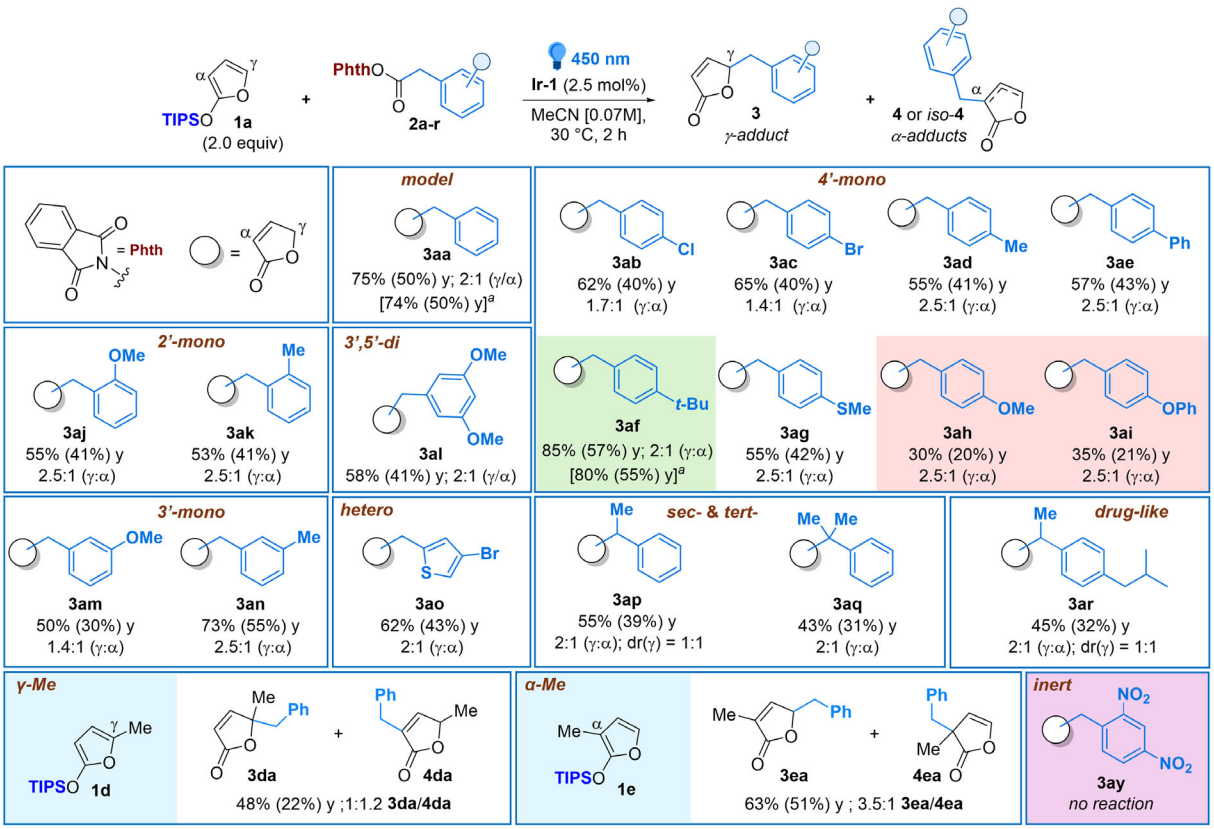

Scheme 3. All reactions were performed using: **1** (0.28 mmol, 2.0 equiv), **2** (0.14 mmol, 1.0 equiv), and **Ir-1** (2.5 mol%) irradiated with blue LEDs (450 nm) in degassed MeCN [0.07M] at 30 °C for 2 h. Combined NMR yields (y) of **3** and *iso*-**4** as revealed by ^{1}H NMR of the crude with trimethylorthoformate as internal standard. In parentheses the isolated yield of pure **3**. In all cases, only the conjugated α-adducts **4** were isolated after chromatographic purification. γ:α ratio was assessed by ^{1}H NMR of the reaction crude. [a]Reaction scaled up on a 3 mmol scale of **2**.

highly electron-deficient 2,4-dinitrobenzyl derivative **2y** was also tested: however, it failed to produce the corresponding butenolide **3ay** under the optimized reaction conditions.

2.3. Protocol B: Reaction Development

Being the 4-hydroxybenzyl moiety a group embedded in many bio-relevant phenyl γ-valerolactone metabolites, the inferior performance observed for **3ah** and **3ai** with Protocol A prompted us to investigate reaction conditions more fitted for such electron-rich substrates (**Table 2**). To this end, we embarked on a second screening of catalysts and conditions focused on optimizing the photoinduced benzylation of **1a** with **2h**. Surprisingly, among the photocatalysts tested, *fac*-Ir(ppy)$_3$ (**Ir-2**) performed at best (Table 2, entry 3), yielding a 1:0.3 **3ah**:*iso*-**4ah** mixture of adducts with a promising 40% NMR combined yield (30% isolated yield of the sole γ-adduct). As for the previous screening, driving the reaction in CD_3CN (Table 2, entry 7) allowed us to follow the reaction progression by ^{1}H NMR. We acknowledged a slower rate as compared to the previous one: indeed, the reaction carried out for 16 h performed well with a sensible improvement in the yield (55%). In line with previous results, we detected phthalimide **7** and bis-adduct **8** and as the main by-products of the reaction, a preliminary proof of the formation of benzyl radical intermediates. To our delight, keeping the reaction for 16 h, under slightly more concentrated conditions [0.1 M], and reverting the **1a**:**2h** stoichiometry to 1:2 proved a smart option, providing a 1:0.25 **3ah**:**4ah** mixture of adducts with a rewarding 88% combined yield (70% isolated yield for the sole **3ah**, Table 2, entry 9).

2.4. Protocol B: Evaluation of Substrate Scope

Under the optimized reaction conditions, a small panel of electron-rich NHPI esters, differently substituted at the 2′- 3′- and 4′-positions, were tested as reaction partners in the radical benzylations of **1a** (**Scheme 4**).

Overall, Protocol B performed better than Protocol A on these substrates in terms of both efficiency and γ versus α regiocontrol. Among all electron-rich, radical precursors tested, the best performances were achieved by benzyl substrates bearing a 4′-OMe group, as evidenced

© 2025 The Author(s). Advanced Synthesis & Catalysis published by Wiley-VCH GmbH

16154169, 2025, 16, Downloaded from https://advanced.onlinelibrary.wiley.com/doi/10.1002/adsc.70035 by CochraneItalia, Wiley Online Library on [13/01/2026]. See the Terms and Conditions (https://onlinelibrary.wiley.com/terms-and-conditions) on Wiley Online Library for rules of use; OA articles are governed by the applicable Creative Commons License

Table 2. Protocol B: optimization of reaction conditions (selected entries).

Entry[a]	Deviations from the initial conditions	Yield [%][b]	r.r.[c] **3ah**:*iso*-**4ah**:**4ah**
1	None	30 (20)	1:0.4:0
2	$Ru(bpy)_3Cl_2$ (**Ru-1**)	<5	n.d.
3	*fac*-Ir(ppy)$_3$ (**Ir-2**)	40 (30)	1:0.3:0
4	**1b** instead of **1a**	20	1:0.5:0
5	**1c** instead of **1a**	35	1:0.5:0
6	**Ir-2** for 16 h	58 (45)	1:0:0.3
7	**Ir-2**, CD_3CN; 16 h	55	1:0:0.4
8	**Ir-2**, 16 h, 1:1 **1a**/**2h**	65	1:0:0.3
9	**Ir-2**, 16 h; 1:2 **1a**/**2h**, [0.1M]	88 (70)	1:0:0.25
10[d]	No photocatalyst nor light	0	n.d.

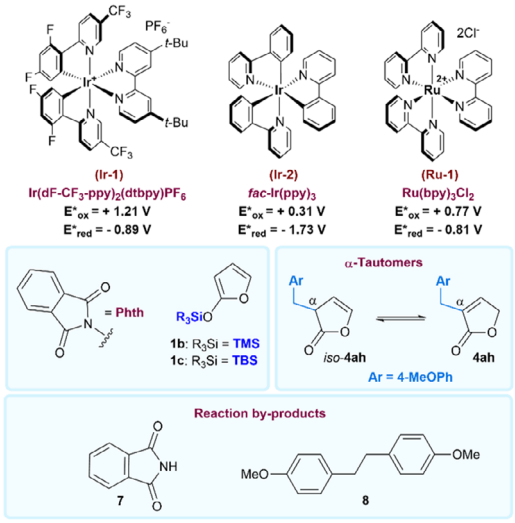

[a] Initial reaction conditions: **1a** (2.0 equiv); **2 h** (0.14 mmol, 1 equiv) and **Ir-1** (2.5 mol%) in degassed MeCN [0.07 M] at 30 °C irradiated with blue LEDs (450 nm) for 2 h;
[b] Combined NMR yield, determined by ^{1}H NMR analysis of the crude with trimethylorthoformate as internal standard. Isolated yield of pure **3ah** in parentheses;
[c] Regioisomeric ratio (r.r.) determined by ^{1}H NMR of the crude;
[d] Reactions performed independently without blue LEDs or without photocatalyst. n.d. = not determined. For details, see Table S6–S10, Supporting Information.

by adducts **3av**, **3aw**, and **3ax**, which were obtained in good 50–75% combined NMR yields (45–60% isolated yields of pure γ-adducts) and with good regiocontrol (from 2.5:1 to 4:1 γ/α ratios). One result was particularly rewarding, namely, the 2′,4′-dimethoxybenzyl derivative **3au**, which stood out as a unicum, since it was obtained almost quantitively as the sole γ-adduct. Interestingly, under Protocol B conditions, benzyl-NHPI ester **2a** and several other electron-poor congeners such as the 4′-Br-benzyl derivative **2c** failed to react with **1a**, clearly indicating a distinct pathway with respect to the reaction promoted by **Ir-1** (vide infra). Furthermore, methylated furans **1d** and **1e** also proved viable substrates for **2h**: indeed, γ-methylfuran **1d** reacted with **2h** to afford a 2.5:1 γ:α mixture of adducts **3dh** and *iso*-**4dh** with 65% combined yield (50% isolated yield of the sole γ-adduct **3dh**, bearing a quaternary carbon center); while its α-methyl congener **1e** yielded the corresponding adducts **3eh** and **4eh** in a rewarding 82% combined yield, albeit with a decreased γ:α regioselectivity (1.7:1 **3eh**/**4eh**). This result, if compared to the behavior of **1e** with Protocol A (Scheme 3), prompted a different mechanism (e.g., a HOMO-driven Mukaiyama-type reaction, vide infra), which could be less susceptible to the steric bias of the methyl group. Finally, as observed with Protocol A, dinitrobenzyl derivative **2y** proved completely inactive.

2.5. Synthetic Utility

The synthetic utility of the disclosed photoinduced benzylation protocols A and B was demonstrated by the accomplishment of a second-generation synthesis of a series of bioactive, chiral hydroxyphenyl-γ-valerolactones PVLs and a 4-(hydroxyphenyl)valeric acid (PVA) scaffold in racemic form (**Scheme 5**). Some years ago, we succeeded in developing an asymmetric entry to chiral, enantiopure PVLs starting from 2-silyloxyfuran **1a** and alkoxy-substituted benzaldehydes as common precursors.[24] In that occasion, enantioenriched γ-valerolactone targets were secured in five to six steps, 18–63% overall yields and 82–98% *ee*. Despite the elegance of the catalytic method and the value of the high enantioselectivity reached, the process suffered from several flaws, such as the need for very low temperature (−78 °C) and the "not-easy-to-handle" stoichiometric $SiCl_4$. In addition, despite the apparently simple structure, streamlined procedures to access the corresponding chiral, open chain derivatives PVAs, are quite rare and mainly limited to metabolomic standards scales.[25]

With a plethora of methoxy-substituted γ-benzyl butenolides available via either Protocols A or B (Scheme 3 and 4), the desired lactone targets could have been shortly at hand, via reduction of the C3-C4 double bond of the butenolide (Et_3SiH, Pd/C in MeOH) followed by standard deprotection of the methoxy moieties with BBr_3 (Scheme 5). This plan proved feasible, and different PVLs **9**-**13** were successfully prepared in 3 steps from **1a** and the corresponding radical precursors **2**, in moderate to good overall yields (26–56%). Furthermore, treatment of lactone **9** with potassium trimethylsilanolate[26] enabled access to the potassium salt of the corresponding 4-hydroxy-5-(4-hydroxyphenyl)valeric acid **14**, opening

© 2025 The Author(s). Advanced Synthesis & Catalysis published by Wiley-VCH GmbH

16154169, 2025, 16, Downloaded from https://advanced.onlinelibrary.wiley.com/doi/10.1002/adsc.70035 by CochraneItalia, Wiley Online Library on [13/01/2026]. See the Terms and Conditions (https://onlinelibrary.wiley.com/terms-and-conditions) on Wiley Online Library for rules of use; OA articles are governed by the applicable Creative Commons License

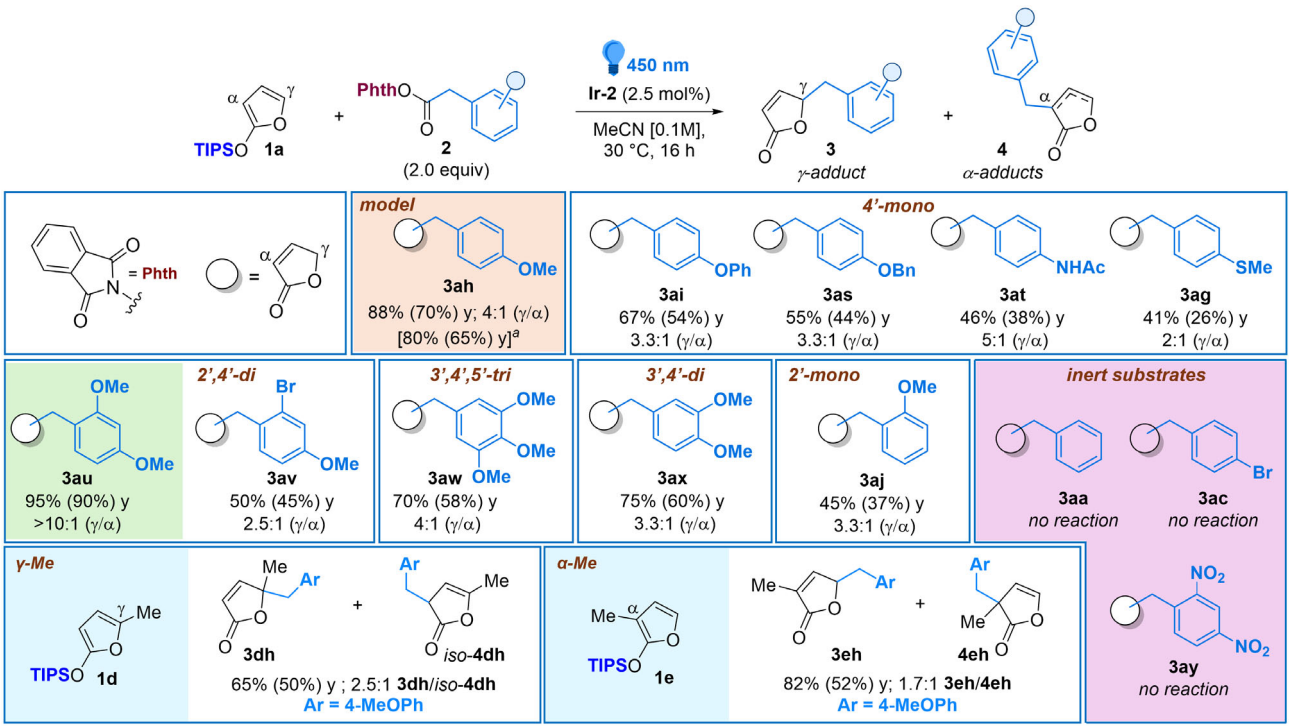

Scheme 4. All reactions were performed using: **1** (0.25 mmol); **2** (2.0 equiv), and **Ir-2** (2.5 mol%), irradiated with blue LEDs (450 nm) in degassed MeCN [0.1 M] at 30 °C for 16 h. Combined NMR yields (y) of γ-**3** and α-**4** adducts as determined by ^{1}H NMR of the crude with trimethylorthoformate as internal standard. In parentheses the isolated yield of pure γ-adducts **3**. γ:α ratio was assessed by ^{1}H NMR of the reaction crude. [a]Reaction scaled up to a 1.0 mmol scale of **1a**.

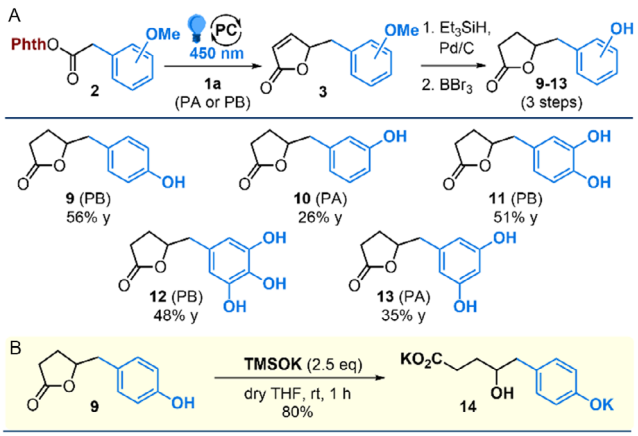

Scheme 5. A) A three-step strategy to access chiral PVLs **9-13.** B) Accessing PVA **14** (potassium salt). PA = Protocol A; PB = Protocol B as outlined in Scheme 3 and 4, respectively. Yield (y) refers to isolated, overall yield for the three-step sequence.

the way to a novel, streamlined access to this class of polyphenol metabolites (Scheme 5B).

2.6. Mechanistic Investigations

Having assessed the synthetic versatility of Protocol A and Protocol B, we next investigated the mechanistic aspects of the disclosed photoinduced benzylations, as applied to model silyloxyfuran **1a** (**Figure 2**). First, cyclic voltammetry (CV) experiments were conducted to determine the redox potentials of key substrates **1a**, **2a**, and **2h** in MeCN (Figure 2A). As expected, **1a** showed an irreversible oxidation wave with a peak potential of +1.17 V (vs Ag pseudoreference), thereby confirming its tendency to be oxidized by photoexcited **Ir-1**. Concerning NHPI esters **2a** and **2h**, in line with other alkyl redox active esters (see Section S7.1, Supporting Information), a couple of similar reductive waves were produced with peak potentials −1.48 and −1.46 V, respectively. We then moved to a series of TEMPO-trapping experiments under protocols A and B, to elucidate the nature of the radical species involved in the reaction (Figure 2B,D). First, treatment of **1a** with 2.0 equivalents of 2,2,6,6-tetramethylpiperidine 1-oxyl radical (TEMPO), with or without the NHPI ester **2a** yielded the corresponding γ-adduct **15** as the sole product in near-quantitative yield (Figure 2B, entries 1 and 2).

In turn, complete inertia was recorded when the same reaction was conducted on the radical precursor **2a** alone, or without light or **Ir-1** (entries 3 and 4). These results, together with the appropriate Stern–Volmer experiments (Figure 2C, left), which revealed that **1a** is a better quencher of photoexcited **Ir-1** than **2a**, clearly

© 2025 The Author(s). Advanced Synthesis & Catalysis published by Wiley-VCH GmbH

16154169, 2025, 16, Downloaded from https://advanced.onlinelibrary.wiley.com/doi/10.1002/adsc.70035 by CochraneItalia, Wiley Online Library on [13/01/2026]. See the Terms and Conditions (https://onlinelibrary.wiley.com/terms-and-conditions) on Wiley Online Library for rules of use; OA articles are governed by the applicable Creative Commons License

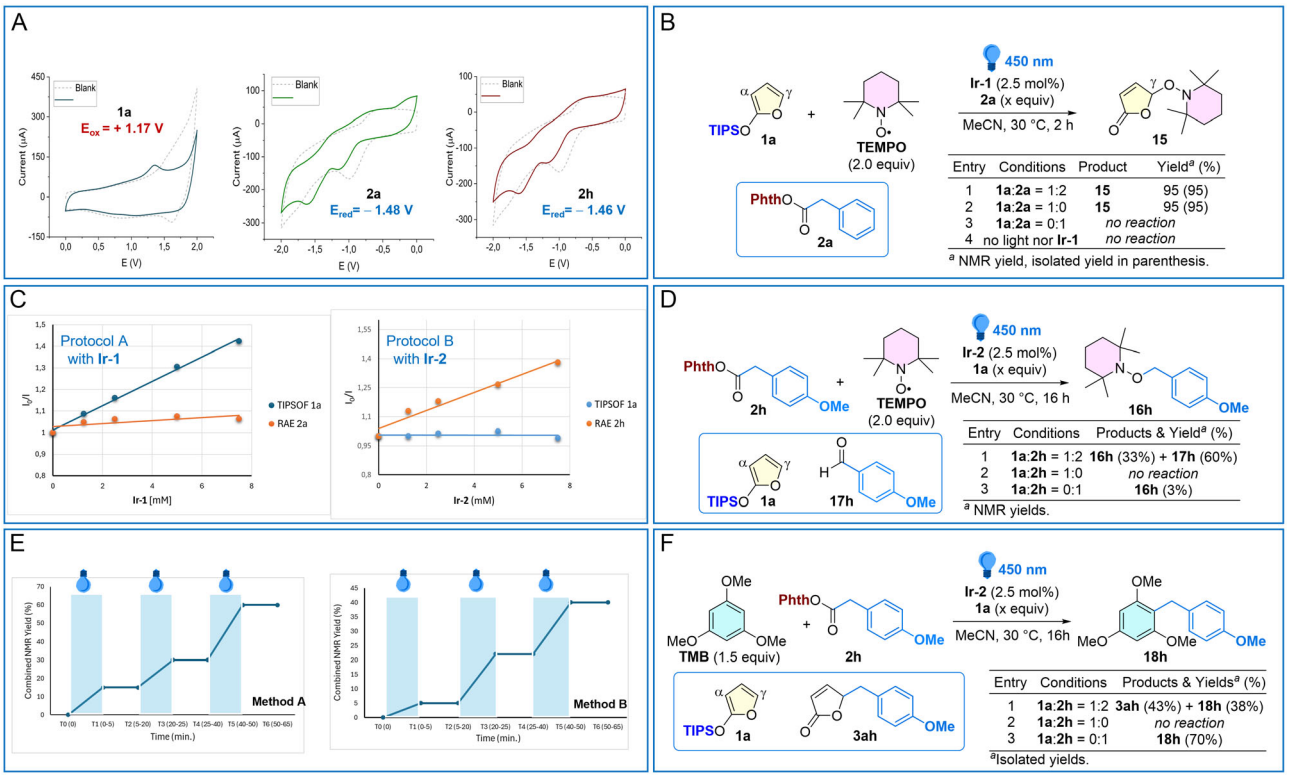

Figure 2. Mechanistic insights and control experiments to support the proposed mechanisms. A) CV Experiments ($E_{1/2}$ = V vs Ag pseudoreference, MeCn). B) Protocol A: Control experiments with TEMPO. C) Stem–Volmer quenching studies. D) Protocol B: Control experiments with TEMPO. E) On–Off experiments. F) Protocol B: Control experiments with 1, 3, 5-trimethoxybenzene (TMB).

suggest that, with Protocol A, silyloxyfuran **1a** is oxidized by **Ir-1** to the expected (silyl) radical cation **1**$^{\bullet+}$. Turning to Protocol B, we tested the reaction between **1a** and the 4-methoxybenzyl derivative **2h** in the presence of TEMPO (2.0 equiv, Figure 2D). Here, after 16 h at 30 °C, we detected the formation of benzyl-TEMPO adduct **16h** (33%) together with 4-methoxybenzaldehyde **17h** as the main product (60% NMR yield, entry 1). Note that no reactivity was observed with **1a** alone (entry 2), whereas compound **16h** was detected but in traces when **2h** was reacted with TEMPO without **1a** (entry 3). In addition, a Stern–Volmer quenching study (Figure 2C, right) revealed that **2 h** is a better quencher for excited **Ir-2** than **1a**, suggesting a quite different mechanism with respect to **Ir-1**. A series of experiments were then carried out in the presence of carbocation quencher 1,3,5-trimethoxybenzene (TMB) as described in Figure 2F. Indeed, treatment of **1a** with **2h** under the conditions of Protocol B, using 1.5 equivalents of TMB and catalytic **Ir-2**, yielded adduct **18h** in a 38% yield along with the corresponding γ-adduct **3ah** (Figure 2F, entry 1). No reaction was observed in the absence of **2h** (entry 2), which in turn reacted properly with TMB in the absence of **1a**, affording the corresponding adduct **18h** in a 70% isolated yield (entry 3). These results agree with the formation of a strongly electrophilic, benzyl carbocation intermediate **2h**$^{+}$ by suitable oxidation of **2h**$^{\bullet}$, unveiling a plausible radical-polar crossover pathway for Protocol B (vide infra). Finally, On–Off experiments (Figure 2E) revealed that no conversion occurred in the dark, and reactions resumed in the presence of light, showcasing the requirement for continuous light irradiation, and suggesting catalytic cycles instead of a radical chain as operative pathways for the disclosed reactions. Notably, these results were also corroborated by the very low quantum yields determined for the two processes: $\Phi = 0.02$ for Protocol A, and $\Phi = 0.05$ for Protocol B (see the Supporting Information).

With all this data at hand, two plausible catalytic cycles were formulated. For the reactions triggered under Protocol A (**Scheme 6A**), a reductive quenching cycle would be operative: here, the photoexcited **Ir-1(III)*** ($E^*_{ox} = +1.21$ V)[21] oxidizes **1a** ($E^*_{ox} = +1.17$ V) to the radical-cation **1a**$^{\bullet+}$ which could react as such or, it might undergo rapid desilylation (by MeCN or phthalimide anion) to the corresponding furanone radical γ-**I**$^{\bullet}$ in resonance with α-**I**$^{\bullet}$. Such radical species then secure formation of products **3** by coupling to the benzyl radical **2**$^{\bullet}$, generated in situ via decarboxylative reduction of benzyl NHPI esters **2** mediated by **Ir-1(II)** hence closing the cycle. On the other hand, the reaction under Protocol

© 2025 The Author(s). Advanced Synthesis & Catalysis published by Wiley-VCH GmbH

16154169, 2025, 16, Downloaded from https://advanced.onlinelibrary.wiley.com/doi/10.1002/adsc.70035 by CochraneItalia, Wiley Online Library on [13/01/2026]. See the Terms and Conditions (https://onlinelibrary.wiley.com/terms-and-conditions) on Wiley Online Library for rules of use; OA articles are governed by the applicable Creative Commons License

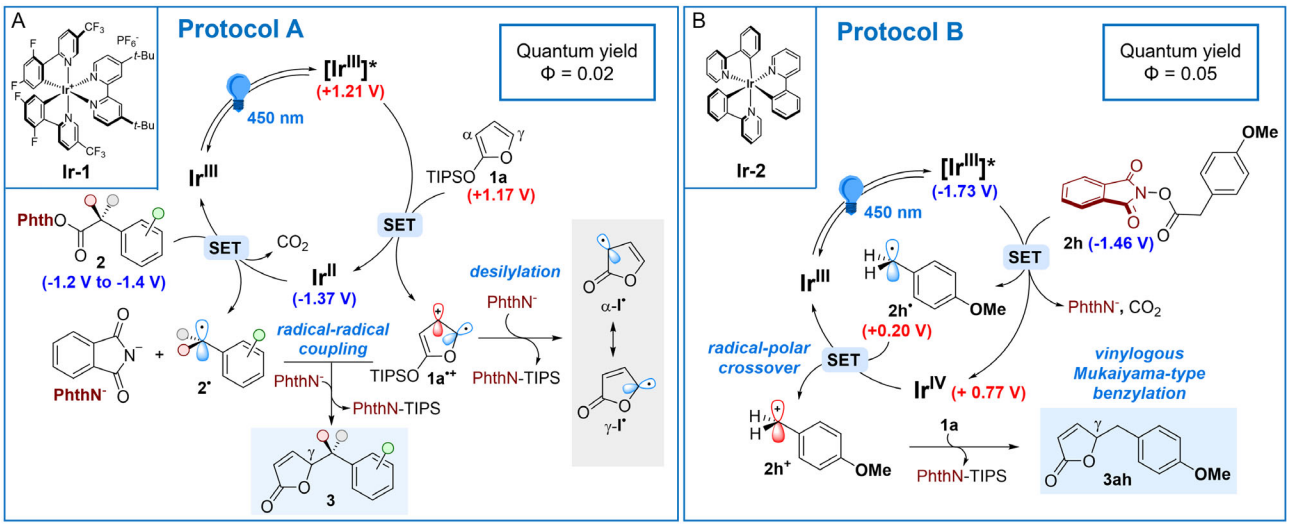

Scheme 6. A) Proposed catalytic cycle for Protocol A. B) Proposed catalytic cycle for Protocol B, as exemplified by **2h**. All reported redox potentials (E_{ox} in red and E_{red} in blue) refer to $E_{1/2}$ = V versus Ag as pseudoreference or SCE in MeCN, see ref. [21] and Section S7.2, Supporting Information.

B (Scheme 6B) seems to be promoted by a net-neutral, radical polar crossover mechanism.[20] Here, the decarboxylative reduction of **2h** ($E_{red} = -1.46$ V) operated by photoexcited **Ir-2** ($E^*_{red} = -1.73$ V)[21] occurs first, generating the corresponding radical intermediate **2h•** which undergoes facile oxidation to the corresponding benzyl carbocation **2h**$^+$ due to the presence of a strong electron-donating group at the *para*-position. This is corroborated by the reported redox potential of the 4-methoxybenzyl radical **2h•** (+0.26 V vs SCE;[19] +0.20 V vs Ag as pseudoreference, see section S7.1.8, Supporting Information) and similar electron-rich congeners, whose oxidation to the corresponding carbocations by **Ir-2(IV)** (+0.77 V)[21] is feasible and might help closing the photoredox oxidative quenching cycle. A Mukaiyama-type, polar, vinylogous benzylation reaction between **1a** and **2h**$^+$ would finally generate the observed benzyl-substituted butenolide **3ah**.

2.7. Computational Analysis

To gain insight into the mechanism of Protocol A, we wondered which actual species would be responsible for the observed reactivity and γ/α regioselectivity, under the optimized reaction conditions. A series of density functional theory calculations were hence performed[27] to elucidate the electronic distribution of triisopropylsilyloxy furan **1a**, its silyl radical-cation **1a**$^{\bullet+}$, and the furanone radical **I•** in terms of HOMO/SOMO orbitals composition, spin density distribution, and Fukui's indices (**Figure 3B,D**). Additionally, global and local electrophilicity and nucleophilicity indices were used to investigate the reactivity of the studied (silyl) furanone radicals (Figure 3A). As evidenced in Figure 3A, while the furanone radical **I•** resulted as a more prominent nucleophilic species ($\omega^0 = 5.1$ vs $N^0 = 8.5$, entry 5), the triisopropylsilyl radical cation **1a**$^{\bullet+}$ appeared to be rather amphiphilic, with a more pronounced electrophilic character ($\omega^0 = 8.5$ vs $N^0 = 7.1$, entry 2). Very similar results were obtained also for the trimethylsilyl radical-cation **1b**$^{\bullet+}$ ($\omega^0 = 8.3$ vs $N^0 = 6.9$, entry 4, see the Supporting Information), unveiling an unprecedented umpolung reactivity when switching from HOMO- to SOMO-driven reactivity of silyl ketene acetals **1**. Since the benzylic radical coupling partners **2** used in Protocol A display a more evident nucleophilic character, especially those bearing EDG substituents,[16] it is highly likely that the radical cations **1**$^{\bullet+}$ serve as more competent reaction partners compared to radical **I•**.

This suggests that the radical coupling event would precede the desilylation step in the catalytic cycle of protocol A (Scheme 6).[28] Regarding the observed regioselectivity, the analysis of molecular orbitals composition, spin density distribution and condensed Fukui indices at radical centers (f_0) for both the triisopropylsilyl radical-cation **1a**$^{\bullet+}$ and the furanone radical **I•** (Figure 3C,D) revealed that the radical center is preferentially located at C5, showing a slight preference for the γ-addition, consistent with experimental observations. Finally, as expected, the neutral, closed-shell triisopropylsilyloxy furan **1a** exhibited a strongly pronounced nucleophilic character ($\omega^0 = 0.7$ vs $N^0 = 3.3$, entry 1 in Figure 3A), supporting its known reactivity in trapping electrophilic carbocations, as in Protocol B. Both HOMO orbital composition analysis and condensed Fukui indices (f^-), once again, revealed a slight preference for the γ-addition (Figure 3B). Not surprisingly, very similar results were obtained also for the trimethylsilyloxy furan **1b** ($\omega^0 = 0.7$ vs $N^0 = 3.4$, entry 3 in Figure 3A).

© 2025 The Author(s). Advanced Synthesis & Catalysis published by Wiley-VCH GmbH

16154169, 2025, 16, Downloaded from https://advanced.onlinelibrary.wiley.com/doi/10.1002/adsc.70035 by CochraneItalia, Wiley Online Library on [13/01/2026]. See the Terms and Conditions (https://onlinelibrary.wiley.com/terms-and-conditions) on Wiley Online Library for rules of use; OA articles are governed by the applicable Creative Commons License

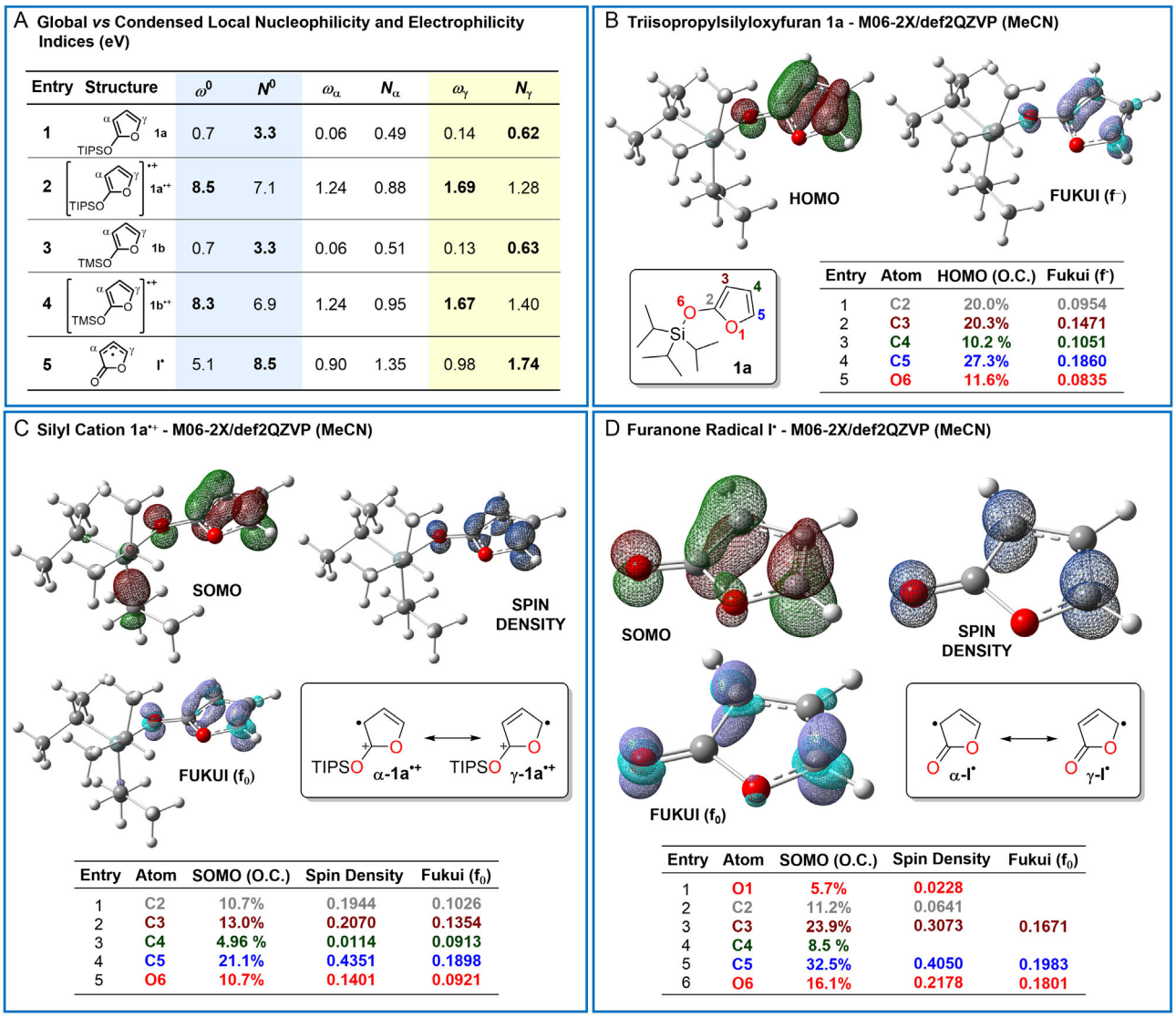

Figure 3. A) Calculated global and condensed local electrophilicity and nucleophilicity indices: N^0 = global nucleophilicity index (eV); ω^0 = global electrophilicity index (eV). N_α, N_γ = Condensed nucleophilicity indices relative to C3 (α) and C5 (γ), respectively. ω_α, ω_γ = Condensed electrophilicity indexes relative to C3 (α) and C5 (γ), respectively. B) Calculated HOMO and Fukui's electronic distribution (f^-) of **1a**. C) SOMO, spin-density population and Fukui's electronic distribution (f_0) of the silyl radical cation $\mathbf{1a}^{\bullet+}$. D) SOMO, spin-density population and Fukui's electronic distribution (f_0) of furanone radical $\mathbf{I}^{\bullet}$.

3. Conclusion

The first, general and vinylogous γ-benzylation reaction of silyloxyfurans **1** with *N*-(arylacetoxy)phthalimides **2** has been accomplished through the implementation of two complementary protocols, PA and PB, promoted by visible light and suitable photoredox catalysts. A wide set of differently functionalized benzylated butenolides were accessed in generally good yields in favor of the γ-benzyl adduct of type **3**. The synthetic potential of the disclosed protocols has been showcased by late-stage modification of several alkoxybenzyl butenolide derivatives which were readily converted to a set of bio-valuable hydroxyphenyl-γ-valerolactones and an unprecedented 4-hydroxy-5-(4-hydroxyphenyl)valeric acid derivative. As this study demonstrates, the amalgamation of polar processes with radical species opened the way to new synthetic opportunities; here, harnessing the principle of vinylogy with radicals emerged as a valuable opportunity to bring new "chemical" life to silyloxyfurans, one of the most exploited vinylogous nucleophile classes in synthesis. Moreover, photoredox catalysis unveiled novel vinylogous reactivity paths: in protocol A, a polarity reversal of the siloxydiene enabled, for the first time, its electron-poor version; in protocol B, polar and radical chemistry merged to blossom an unprecedented vinylogous Mukaiyama-type benzylation reaction. Since this field is currently shaping up,

© 2025 The Author(s). Advanced Synthesis & Catalysis published by Wiley-VCH GmbH

16154169, 2025, 16, Downloaded from https://advanced.onlinelibrary.wiley.com/doi/10.1002/adsc.70035 by CochraneItalia, Wiley Online Library on [13/01/2026]. See the Terms and Conditions (https://onlinelibrary.wiley.com/terms-and-conditions) on Wiley Online Library for rules of use; OA articles are governed by the applicable Creative Commons License

there is a lot more that needs to be explored, especially in terms of the broad scope of compatible vinylogous nucleophiles and electrophiles to be used in conjunction with suitable radical counterparts. Overall, we believe that the disclosed strategies will become more widely employed and will emerge as a powerful tool in synthetic organic chemistry.

Acknowledgements

This work has been carried out in the frame of the ALIFAR project, funded by the Italian Ministry of University through the program "Dipartimenti di Eccellenza 2023-2027," and granted by the University of Parma through the action Bando di Ateneo 2022 per la ricerca co-funded by MUR-Italian Ministry of Universities and Research - D.M. 737/2021 - PNR - PNRR – NextGenerationEU. M.G. and S.F. have benefited from the equipment and framework of the COMP-R Initiative, funded by the "Departments of Excellence" program of the Italian Ministry for University and Research (MUR, 2023-2027). L.A. acknowledges funding of his Ph.D. grant by Dr. Francesco Casiraghi, in memory of his beloved father Prof. Giovanni Casiraghi. M.L. acknowledges the University of Bologna (RFO) for financial support. E.M. acknowledges funding by the EU PRIMA program (MED4Youth project), supported by the "Ministero dell'Istruzione, dell'Università e della Ricerca - MIUR. Sara Dobani and Luca Calani (University of Parma) are greatly acknowledged for technical support with HRMS data. The authors also thank Prof. Dr. Serena Silvi (University of Bologna) for precious support in the determination of the quantum yields.

Open access publishing facilitated by Universita degli Studi di Parma, as part of the Wiley - CRUI-CARE agreement.

Conflict of Interest

The authors declare no conflict of interest.

Data Availability Statement

Research data are not shared

References

[1] To the best of our knowledge, the first work ever published regarding the preparation of a silyloxyfurans is the following: E. Yoshii, T. Koizumi, E. Kitatsuji, T. Kawazoe, T. Kaneko, *Heterocycles* **1976**, *4*, 1663.

[2] a) C. Curti, L. Battistini, A. Sartori, F. Zanardi, *Chem. Rev.* **2020**, *120*, 2448; b) G. Casiraghi, L. Battistini, C. Curti, G. Rassu, F. Zanardi, *Chem. Rev.* **2011**, *111*, 3076; c) G. Casiraghi, F. Zanardi, G. Appendino, *Chem. Rev.* **2000**, *100*, 1929.

[3] B. Mao, M. Fañanás-Mastral, B. L. Feringa, *Chem. Rev.* **2017**, *117*, 10502.

[4] L. Hoppmann, O. García Mancheño, *Molecules* **2021**, *26*, 6902.

[5] T. B. Wright, P. A. Evans, *Chem. Rev.* **2021**, *121*, 9196.

[6] a) F. Richard, S. Aubert, T. Katsina, L. Reinalda, D. Palomas, R. Crespo-Otero, J. Huang, D. C. Leitch, C. Mateos, S. Arseniyadis, *Nat. Synth.* **2022**, *1*, 641; b) For a seminal work reporting an example of polar, vinylogous benzylation of 1b promoted by stoichiometric AgOTf see: K. Takeda, A. Ayabe, H. Kawashima, Y. Harigaya, *Tetrahedron Lett.* **1992**, *33*, 951.

[7] J. Hur, J. Jang, J. Sim, *Int. J. Mol. Sci.* **2021**, *22*, 2769.

[8] P. Mena, L. Bresciani, N. Brindani, I. A. Ludwig, G. Pereira-Caro, D. Angelino, R. Llorach, L. Calani, F. Brighenti, M. N. Clifford, C. I. R. Gill, A. Crozier, C. Curti, D. D. Rio, *Nat. Prod. Rep.* **2019**, *36*, 714.

[9] Selected examples: a) T. Hirata, Y. Ogasawara, S. Kobayashi, Y. Yamashita, *Chem. Asian J.* **2022**, *17*, e202200647; b) T. O. Paulisch, F. Strieth-Kalthoff, C. Henkel, L. Pitzer, D. M. Guldi, F. Glorius, *Chem. Sci.* **2020**, *11*, 731; c) C. Pac, K. Mizuno, H. Okamoio, H. Sakurai, *Synthesis* **1978**, 589.

[10] a) J. Paut, S. Baldon, E. Anselmi, L. Dell'Amico, G. Dagousset, E. Magnier, *Adv. Synth. Catal.* **2024**, *366*, 3500; b) C. Banoun, F. Bourdreux, E. Magnier, G. Dagousset, *Org. Lett.* **2021**, *23*, 8926; c) K. Goliszewska, K. Rybicka-Jasińska, J. Szurmak, D. Gryko, *J. Org. Chem.* **2019**, *84*, 15834.

[11] For a recent, comprehensive review on Photoinduced Electron Transfer (PET) promoted transformations of enol silanes, see: G. Yue, B. Liu, *Tetrahedron Chem.* **2024**, *9*, 100067.

[12] a) S. Fukuzumi, M. Fujita, J. Otera, Y. Fujita, *J. Am. Chem. Soc.* **1992**, *114*, 10271; b) M. Schmittel, M. Lal, R. Lal, M. Röck, A. Langels, Z. Rappoport, A. Basheer, J. Schlirf, H.-J. Deiseroth, U. Flörke, G. Gescheidt, *Tetrahedron* **2009**, *65*, 10842.

[13] a) J. O. Bunte, E. K. Heilmann, B. Hein, J. Mattay, *Eur. J. Org. Chem.* **2004**, 3535; b) P. G. Gassman, K. J. Bottorff, *J. Org. Chem.* **1988**, *53*, 1097.

[14] The different behavior between a silyl radical cation species and its corresponding desilylated congener has been studied mainly on cyclization reactions. For seminal works on this topic, see: a) M. Schmittel, M. Kelley, A. Burghart, *J. Chem. Soc., Perkin Trans.* **1995**, *2*, 2327; b) A. Heidbreder, J. Mattay, *Tetrahedron Lett.* **1992**, *33*, 1973; c) B. B. Snider, T. Kwon, *J. Org. Chem.* **1992**, *57*, 2399.

[15] a) J. Zhang, M. Liu, W. Zhang, C. Guo, *Sci. Adv.* **2025**, *11*, eadu5594; b) C. Banoun, F. Bourdreux, G. Dagousset, *Chem. Commun.* **2023**, *59*, 760; c) K. F. Szabó, K. Goliszewska, J. Szurmak, K. Rybicka-Jasińska, D. Gryko, *Org. Lett.* **2022**, *24*, 8120; d) M. Briand, L. D. Thai, F. Bourdreux, N. Vanthuyne, X. Moreau, E. Magnier, E. Anselmi, G. Dagousset, *Org. Lett.* **2022**, *24*, 9375; e) M. Balletti, E. Marcantonio, P. Melchiorre, *Chem. Commun.* **2022**, *58*, 6072; f) Also, for a seminal work on a non-photoinduced SET oxidation of linear silyl dienol ethers see: B. Paolobelli, D. Latini, R. Ruzziconi, *Tetrahedron Lett.* **1993**, *34*, 721.

© 2025 The Author(s). Advanced Synthesis & Catalysis published by Wiley-VCH GmbH

16154169, 2025, 16, Downloaded from https://advanced.onlinelibrary.wiley.com/doi/10.1002/adsc.70035 by CochraneItalia, Wiley Online Library on [13/01/2026]. See the Terms and Conditions (https://onlinelibrary.wiley.com/terms-and-conditions) on Wiley Online Library for rules of use; OA articles are governed by the applicable Creative Commons License

[16] For notable accounts of the concept of radical philicity see: a) J. J. A. Garwood, A. D. Chen, D. A. Nagib, J. Am. *Chem. Soc.* **2024**, *146*, 28034; b) F. Parsaee, M. C. Senarathna, P. B. Kannangara, S. N. Alexander, P. D. E. Arche, E. R. Welin, *Nat. Rev. Chem.* **2021**, *5*, 486; c) For a recent example related to electronically mismatched radical additions to alkenes, see: S. Paul, D. Filippini, M. Silvi, *J. Am. Chem. Soc.* **2023**, *145*, 2773.
[17] J. D. Bell, J. A. Murphy, *Chem. Soc. Rev.* **2021**, *50*, 9540.
[18] a) S. K. Parida, T. Mandal, S. Das, S. K. Hota, S. De Sarkar, S. Murarka, *ACS Catal.* **2021**, *11*, 1640; b) M. A. Syroeshkin, I. B. Krylov, A. M. Hughes, I. V. Alabugin, D. V. Nasybullina, M. Y. Sharipov, V. P. Gultyai, A. O. Terent'ev, *J. Phys. Org. Chem.* **2017**, *30*, e3744.
[19] For accounts on the redox potentials of substituted benzyl radicals, see: a) K. Ishiguro, T. Nakano, H. Shibata, Y. Sawaki, *J. Am. Chem. Soc.* **1996**, *118*, 7255; b) B. A. Sim, P. H. Milne, D. Griller, D. D. M. Wayner, *J. Am. Chem. Soc.* **1990**, *112*, 6635.
[20] R. J. Wiles, G. A. Molander, *ISR. J. Chem.* **2020**, *60*, 281.
[21] C. K. Prier, D. A. Rankic, D. W. C. MacMillan, *Chem. Rev.* **2013**, *113*, 5322.
[22] A. Tlahuext-Aca, R. A. Garza-Sanchez, F. Glorius, *Angew. Chem. Int. Ed.* **2017**, *56*, 3708.
[23] For a recent, non-photoinduced dimerization of siloxydienes via an oxidative pathway see: D. Galaktionova, X. Liu, X. Chen, J. T. Mohr, *Chem. Eur. J.* **2024**, *30*, e202302901.
[24] C. Curti, N. Brindani, L. Battistini, A. Sartori, G. Pelosi, P. Mena, F. Brighenti, F. Zanardi, D. Del Rio, *Adv. Synth. Catal.* **2015**, *357*, 4082.
[25] M. Mülek, A. Fekete, J. Wiest, U. Holzgrabe, M. J. Mueller, P. Högger, *J. Pharm. Biomed. Anal.* **2015**, *114*, 71.
[26] E. D. Laganis, B. L. Chenard, *Tetrahedron Lett.* **1984**, *25*, 5831.
[27] The geometries of all compounds under scrutiny were fully optimized by using the dispersion corrected M06-2X hybrid functional with the def2qzvp basis set, implemented in the Gaussian 16 package. The solvent effect was considered using the IEFPCM continuum solvation model in acetonitrile (MeCN). Conceptual Density Functional Theory (CDFT) analyses were done using the open-source post-processing software Multiwfn32 on the fully optimized geometries (M06-2X/def2qzvp/IEFPCM = MeCN). Electrophilicity indices ω were calculated as $\mu^2/(2\eta)$ using the values of vertical ionization potential and vertical electron affinity. Nucleophilicity indices N were calculated as $E_{HOMO} - E_{HOMO(TCE,\ tetracyanoethylene)}$ for neutral molecules, and as $E^{\alpha}_{HOMO} - E^{\alpha}_{HOMO(F\bullet)}$ for radical species. (See refs. 43-49 in the Supporting Information).
[28] Despite this evidence, we cannot rule out the possibility that furanone radical I• might be the species involved in the radical coupling step of Protocol A. Indeed, two observations would corroborate this hypothesis: a) the known, "fast" desilylation step of silylenol ethers in MeCN, and b) the complete γ-selectivity observed with TEMPO radical, which probably involves radical cation $1a^{\bullet+}$ (Figure 2b).

© 2025 The Author(s). Advanced Synthesis & Catalysis published by Wiley-VCH GmbH

16154169, 2025, 16, Downloaded from https://advanced.onlinelibrary.wiley.com/doi/10.1002/adsc.70035 by CochraneItalia, Wiley Online Library on [13/01/2026]. See the Terms and Conditions (https://onlinelibrary.wiley.com/terms-and-conditions) on Wiley Online Library for rules of use; OA articles are governed by the applicable Creative Commons License